Electronic energy transfer in Na2

A. G. Astill, A. J. McCaffery, S. C. Taylor, B. J. Whitaker, and M. J. Wynn

Citation: The Journal of Chemical Physics **89**, 184 (1988); doi: 10.1063/1.455502
View online: http://dx.doi.org/10.1063/1.455502
View Table of Contents: http://scitation.aip.org/content/aip/journal/jcp/89/1?ver=pdfcov
Published by the AIP Publishing

Electronic energy transfer in Na_2

A. G. Astill, A. J. McCaffery, S. C. Taylor, B. J. Whitaker, and M. J. Wynn
School of Chemistry and Molecular Sciences, University of Sussex, Falmer, Brighton BN1 9QJ, England

(Received 2 October 1987; accepted 15 March 1988)

The emission spectrum of the $A\ ^1\Sigma_u^+ - X\ ^1\Sigma_g^+$ band of Na_2 has been recorded following both multimode and single mode excitation of the $B\ ^1\Pi_u$ state using an argon ion laser. The spectral profile has been investigated as a function of excitation frequency, cell temperature and buffer gas pressure. Simulation of the band profile shows that the $A\ ^1\Sigma_u^+$ state is vibrationally inverted. This is interpreted through a populating mechanism involving collisional transfer from the $B\ ^1\Pi_u$ to the (2) $^1\Sigma_g^+$ state followed by radiative transfer to the $A\ ^1\Sigma_u^+$ state. The collision partner is most likely to be ^2S state Na atoms. The emission is also found to be significantly negatively polarized with respect to the laser polarization plane. The results are discussed in the light of various theoretical models.

I. INTRODUCTION

Until the recent upsurge of interest in experiments on electronic energy transfer at the state-to-state level, very few precise data were available on this phenomenon. Energy transfer between electronic terms can occur in an isolated molecule if the density of states is high, however in small molecules this is not usually the case and here the interconversion proceeds as a result of the interaction of the molecule with its environment. For molecules in the gas phase two types of collisional mechanisms have been proposed. The earliest of these is the "gate" model in which collisional perturbations cause mixing through nonadiabatic coupling (e.g., spin–orbit, orbit–rotation) in the free molecule leading to inelastic transitions between the rotational manifolds of the two Born–Oppenheimer electronic states.[1–5] Since a perturbed level is the (time dependent) superposition of the mutually perturbing states this energy transfer mechanism is essentially a form of rotational energy transfer. The other mechanism, which has been proposed more recently, relies on the realization that the approach of a collision partner will lift the cylindrical symmetry of the molecule (except for collinear approach) and allow electrostatic coupling to occur between the electronic states. This has the effect of inducing "optical-like" dipolar transitions between rovibrational levels of the two surfaces, and is "pure" inelastic energy transfer.[6]

Previous experimental studies have examined $^2\Pi$–$^2\Sigma$ surface crossings in systems such as CaO,[5] CN,[9,11–14] N_2^+,[3,7,8] and N_2,[10] in collision with the rare gases. Particularly noteworthy are the rotationally resolved studies of Dagdigian and co-workers[11–14] on the CN radical and of Katayama[8] on the N_2 positive ion. Electronic energy transfer is also known to occur in the alkali diatomics from the observation of A–X band fluorescence in both Li_2 and Na_2 following laser excitation into the B state.[15–18] Work using Fourier transform infrared (FTIR) spectroscopy by Effantin *et al.*[17] has given information on the role of the recently discovered (2) $^1\Sigma_g^+$ state of Na_2,[19] which crosses the $B\ ^1\Pi_u$ state, in the electronic energy transfer process.

In this paper we present a detailed study of the $A\ ^1\Sigma_u^+ - X\ ^1\Sigma_g^+$ fluorescence in Na_2 following excitation into the $B\ ^1\Pi_u$ state using lines from an Ar^+ laser. Results have been obtained for both multimode and single mode operation. The A–X fluorescence has been modeled using a simulation which demonstrates that the A state population is vibrationally inverted. This result may also be deduced from the FTIR spectra obtained by Effantin *et al.*[17] We also report the results of an experiment designed to map out the $B\ ^1\Pi_u$–(2) $^1\Sigma_g^+$ crossing as a function of the initially populated rovibrational level. From these results we comment on various possible crossing mechanisms which have been proposed.

II. EXPERIMENTAL

The experimental arrangement is shown in Fig. 1. An Ar^+ laser (Spectra Physics model 165) was used to excite selected rovibrational lines in the X–B band of Na_2 vapor. The laser was fitted with an intracavity air spaced etalon (Spectra Physics model 589-12) to allow single mode operation. Sodium vapor, of which about 1% is in dimer form, was contained in a stainless steel cell fitted with five viewing/access ports arranged perpendicularly to each other. The cell design is based on a commercially available six-way cross vacuum fitting in which one of the six arms is used for heat-

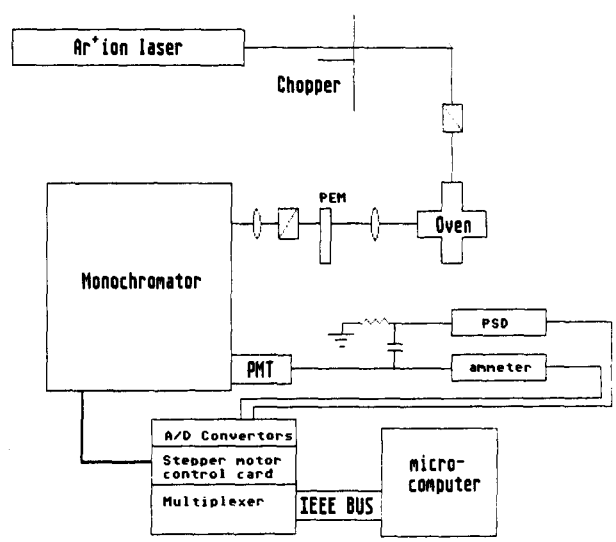

FIG. 1. The experimental setup.

 0021-9606/88/130184-08$02.10

ing purposes while the other five allow viewing and laser access. Heating is achieved using two commercial 600 W cartridge heaters (Hedin model CP 3229) inserted externally into a stainless steel block which in turn is welded into the sixth arm of the cell. A chromel/alumel thermocouple is placed in the block to provide a temperature measurement. The output of the thermocouple is also used in a thermostatic controller which maintains the cell at the required temperature, typically around 750 K. The top of the block is machined to form a crucible which then holds the molten sodium. Conical baffles (three per arm) can be placed into the laser access arms to reduce the light scatter. Finally a stainless steel chimney, which is pierced by four 4 mm holes along the axes of the horizontal arms, can be placed in the center of the cell. The advantages of this cell design over a conventional heat pipe type result from increased flexibility in terms of fluorescence collection and laser access. Sodium vapor stability is also increased as the sodium refluxes in the central arm, this also reduces condensation on the colder surfaces of the cell and enhances the time between refills of the cell. Furthermore the cell can be operated at very low pressures of an inert buffer gas to maintain a central column of vapor.

The fluorescence from the excited Na_2 molecules was collected at right angles to the laser propagation direction and focused on to the entrance slit of a double grating monochromator (Coderg model PH1). The maximum attainable resolution was 0.5 cm^{-1} but most of the spectra were recorded at a resolution of 4 cm^{-1}. A cooled photomultiplier (PM) tube (EMI model 9658B:S20 response) was placed after the exit slit of the monochromator. The output of the PM tube was measured using a phase sensitive detector (PSD) (Stanford Research model SR510) with the laser modulated at $\sim$5 kHz by a mechanical chopper (HMS model 220A). The output from the PSD was converted into a 12 bit digital signal and recorded via a Microlink computer interface (Biodata). The grating arm of the monochromator could also be positioned through a stepper motor control module in the interface by minor modification of the spectrometer. The interface itself is controlled by IEEE 488 protocol from a microcomputer (Apricot PC). The entire experiment was controlled by a FORTRAN 77 (Microsoft) program. The spectra were corrected for the nonlinear wavelength response of the detection chain, in particular, the gratings and the PM tube. The correction was done by recording the spectrum of a tungsten white light source. This spectrum was then fitted to the known tungsten emission curve using a cubic spline (20 knot points). Inversion of the spline fit gave the required machine correction function which was then used to weight subsequently recorded spectra.

The final part of the experimental setup consists of the polarization optics; two linear polarizers and a photoelastic modulator (Morvue model MFS 3). Full details of the polarization measurement technique can be found elsewhere[20] so only brief details are included here. The photoelastic modulator (PEM) together with the analyzing polarizer are placed before the monochromator slits. The second linear polarizer is used to "clean up" the laser polarization before it enters the cell. The PEM can be used to provide either full- or half-wave rectification according to the frequency of the driving voltage, and the analyzing polarizer is aligned so that the modulated signal is polarized perpendicularly to the grooves of the gratings. The photocurrent from the PMT is divided by a cross-over circuit which drops the high-frequency component across a load resistor to the input of the PSD, the low-frequency component is sent directly to the input of a picoammeter (Keithley model 414A). The experimental geometry is such that the fluorescence is collected perpendicular to the laser propagation vector (**O**). Consequently linearly polarized excitation has to be used with full-wave rectification of the fluorescent signal. The modulated signal is thus proportional to $I^{\parallel} - I^{\perp}$ while the total photocurrent is proportional to $I^{\parallel} + I^{\perp}$, where $I^{\parallel}$ and $I^{\perp}$ are the intensities of the emitted light polarized parallel and perpendicular to the initial quantization axis. The linear polarization ratio $P = (I^{\parallel} - I^{\perp})/(I^{\parallel} + I^{\perp})$ is a measure of the degree of alignment present in the excited state. The analogous circular polarization ratio $C = (I^{+} - I^{-})/(I^{+} + I^{-})$ where $I^{\pm}$ is the intensity of the ($\pm$) circular polarized emission, is a measure of the degree of orientation present in the excited state. In general circular polarization ratios are larger than corresponding linear ratios, however measurement of C requires the fluorescence to be collected along **O** and we were unable to use this geometry because of poor rejection by the monochromator of scattered laser light due to higher order grating ghosts.

The intensity and form of the emission band has been investigated as a function of the following parameters:

(1) The buffer gas (He and Xe) pressure from 0 to 400 Torr.
(2) Cell temperature in the range 650 to 800 K.
(3) The X–B excitation wavelength (514.5–457.9 nm) initially using the laser multimode but later in single mode.

III. RESULTS

Figure 2 shows a typical fluorescence spectrum before and after correction for the machine function, obtained with the 488.0 nm line of the Ar^{+} laser. This excitation wavelength corresponds to the transition $X\,^1\Sigma_g^+ (v = 3, J = 43) \rightarrow B\,^1\Pi_u (v = 6, J = 43)$. Depending on the temperature of the cell, and consequently on the sodium atom number density, the Na D lines are seen either as sharp emission features or as absorption on the molecular emission background. This latter effect is due to radiation trapping. Atomic emission is mainly the result of electronic quenching by atomic sodium[21];

$$Na_2^*(B\,^1\Pi_u) + Na(3\,^2S_{1/2}) \rightarrow Na(X\,^1\Sigma_g^+) + Na^*(3\,^2P_J),$$

for which the experimental cross section is 4×10^{-15} cm^2.[22] Photofragmentation and predissociation processes may also contribute to the atomic fluorescence.[23]

The molecular spectra show extensive rovibrational structure over the range of the A–X band. To the red of the band profile, sharp "satellite" structure is visible around 12 400 cm^{-1}. This structure appears at the turning point of the potential difference curve and is characteristic of the A–X band.[24] Analysis of the Franck–Condon (FC) factors in-

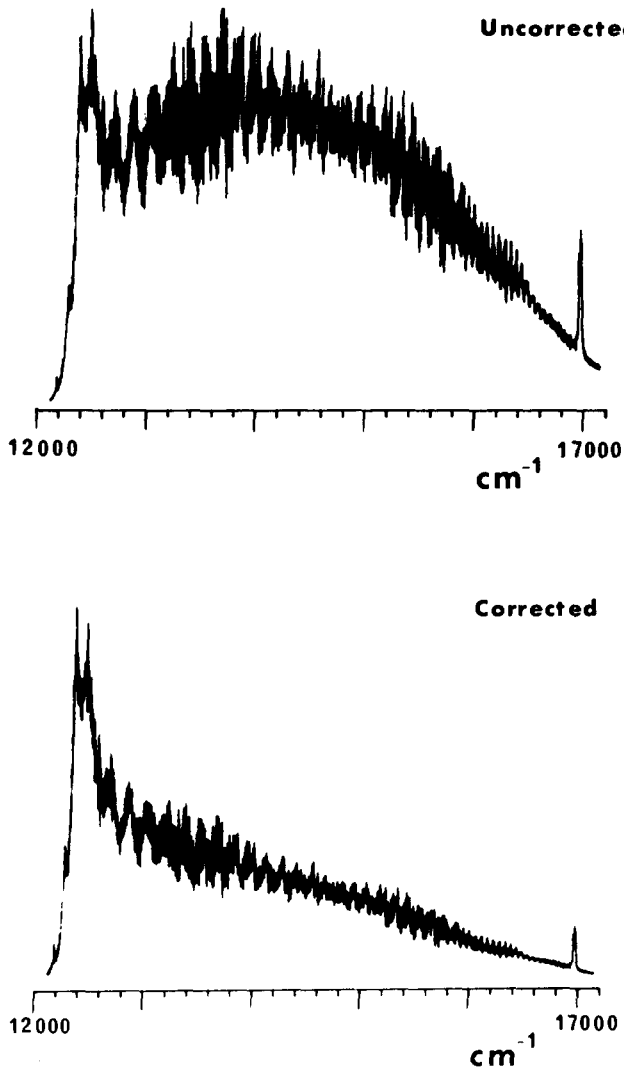

FIG. 2. Observed A–X fluorescence before (upper trace) and after (lower trace) correction for the nonlinear wavelength response of the detection chain. Cell temperature 750 K, 5 Torr He.

dicates that this does not correspond to the most intense transition but to a superposition of many individual, comparatively low intensity transitions.

The emission intensity is found to be independent of buffer gas pressure save for fluorescence quenching which is observed at very high pressures (>100 Torr). This is in contrast to the observations of Ennen and Ottinger,[15] who have studied the analogous emission in the Li_2 molecule. In these latter experiments the A–X emission intensity, following B state excitation, was found to be proportional to buffer gas (Ar) pressure, although the shape of the band was not changed. However these authors did observe pressure independent emission in the B–X band following laser excitation of the $C\,^1\Pi_u$ levels. It is important to stress the fact that the Na_2 A–X emission that we observe is present in the absence of all buffer gas in the laser/metal vapor interaction zone, i.e., under heat piping conditions.

When the band profile of the Na_2 A–X emission was investigated as a function of cell temperature it was found to be essentially independent of temperature, while the intensity was found to be proportional to the Na (and hence the Na_2) pressure. The Na partial pressure is found by reference to the tables of vapor pressure against temperature.[25] We note that this observation is consistent with the data obtained by Pardo *et al.*,[26] who found that the B–X fluorescence was directly proportional to the intensity in the A–X band when measured as a function of laser fluence, and hence concentration of Na_2^*. Unfortunately these workers misinterpreted the A–X spectrum as absorption against some unspecified continuum emission.

The initial multimode laser study showed that the transfer efficiency was dependent on the X–B excitation frequency with the blue lines producing less than the green lines. Figure 2 of Ref. 16 shows these results. The use of an etalon to achieve single mode operation of the laser has allowed us to quantify the transfer rates out of the individual rovibrational levels initially populated. In these experiments the laser was directed through the cell, and the B–X and A–X fluorescent light emerging through one of the side arms of the cell was detected by a photomultiplier tube (EMI model 9558:S20 response) placed behind the exit slits of a 0.25 m grating monochromator (Spex Minimate). The B–X fluorescence was also collected coaxially to the laser and dispersed through the PH1 monochromator. In this way the mode selectivity of the laser could be checked, while making simultaneous measurements of the relative quantum yield in the two bands. The total spectral intensity in each of the bands was obtained by recording the spectra on chart paper and weighing the resultant profiles. The results are shown in Table I. The most efficient transfer is found to occur for excitation to the ($v=12, J=36$) and ($v=10, J=12$) levels of the B state.

A very interesting result is that of the polarization studies. The A–X band profile was found to be significantly negatively polarized ($\sim 10\%$). That is to say excitation into the B state with perpendicular polarization produces emission in the A–X band in which the net polarization is in the parallel plane with respect to the laboratory frame. Although the polarized signal does not exactly mirror the total photocurrent profile, which shows that the lines are not all polarized to the same degree, we were unfortunately unable to obtain

TABLE I. Relative fluorescence quantum yield in the A–X and B–X bands of Na_2 following single mode excitation X–B. Cell temperature 750 K, 5 Torr He.

Excitation $X\,^1\Sigma_g - B\,^1\Pi_u$				$B\,^1\Pi_u$ state energy	Relative quantum yield $(A\text{–}X)/(B\text{–}X)$
v''	J''	v'	J'	cm^{-1}	$\times 10^{-2}$
3	43	6	43	21 319.481	0.93 ± 0.2
4	30	4	30	20 976.201	1.14 ± 0.4
0	28	6	27	21 185.434	1.09 ± 0.4
6	44	7	43[a]	21 436.744	1.18 ± 0.4
5	55	9	56	21 795.579	1.15 ± 0.4
3	13	10	12	21 556.789	1.38 ± 0.2
6	38	5	37	21 148.702	1.24 ± 0.4
3	36	12	36	21 898.724	1.74 ± 0.4

[a] The excitation frequency for the $X(v=6, J=44) \rightarrow B(v=7, J=43)$ transition also partially coexcites the $X(v=7, J=29) \rightarrow B(v=8, J=28)$ transition.

ratios for individual rotational lines. The result however shows that the transfer cross sections depend on the alignment of the molecule with respect to the exciting laser beam propagation direction, i.e., are M_J dependent.

In an attempt to obtain the rotational and vibrational distribution following electronic energy transfer a computer simulation of the A–X emission spectrum was performed. Initial simulations[16] used the expression:

$$I^{\rm em}_{v'v''} = 64/3\pi^4 c\nu^4 \omega_{J'} S_{J'J''} N_{v'} R^2 |\langle \Psi_{v'} | \Psi_{v''} \rangle|^2, \quad (1)$$

where $N_{v'}$ is the population of the excited state v' level, $\langle \Psi_{v'} | \Psi_{v''} \rangle$ is the Franck–Condon (FC) overlap integral, $\omega_{J'}$ accounts for the nuclear spin statistics, $S_{J'J''}$ is the Hönl–London factor, and R is the average dipole moment between the A and X states. This often gives adequate results but is not strictly correct. The Franck–Condon approximation to the exact transition matrix element $\langle \Psi_{v'} | \mathbf{u}\cdot\mathbf{e} | \Psi_{v''} \rangle$ is particularly suspect when the dipole moment varies considerably with internuclear distance as is the case for the A–X band in Na_2. In this work we calculated the required transition moments using a program written by Le Roy[27] and the published variation of $\mu(R)$.[28] The resultant Einstein A coefficients were checked against those of Stevens *et al.*[28] and were found to be in excellent agreement. The potentials used were those of Kusch and Hessel[29] for the X state and Kaminsky[30] for the A state both obtained from RKR fits to experimental data.

The spectrum was simulated for a number of different $N_{v'}$ distributions. For each v' level a thermal rotational distribution was added according to the usual rotational partition function. This is valid since rotational relaxation is generally 100–1000 times faster than vibrational relaxation and consequently the rotational distribution can be taken as completely thermalized at the cell temperature (650–800 K). It should be noted, however, that the transition moments were calculated for $J = 0$ only since evaluation of the matrix elements $\langle \Psi_{v'J'} | \boldsymbol{\mu}\cdot\mathbf{e} | \Psi_{v''J''} \rangle$ would have required extravagant computational resources. Although an examination of the Boltzmann rotational distribution function for the A state showed that about 200 rotational levels should have been included, in order to save computer time the number of J' states included for each v' level was varied from 50 to 200. It was found that increasing the number of states above 75 failed to produce any significant changes in the resultant profile.

The initial choice of N_v was the Boltzmann distribution,

$$N_v = \exp(-\epsilon_v/kT_{\rm vib})/[1 - \exp(-\epsilon_v/kT_{\rm vib})], \quad (2)$$

in view of the broad band nature of the fluorescence. However this function conspicuously failed to reproduce the spectrum for any reasonable value of $T_{\rm vib}$ (500–7000 K). As reported earlier[16] we then attempted to obtain a phenomenological description of the A state vibrational distribution using a Gaussian function of variable width which could be centered on particular vibrational levels

$$N_v = (\alpha/\pi)^{1/2} \exp[-\alpha(v - v_0)^2]. \quad (3)$$

After the data has been corrected for the machine function, the choice of $v_0 = 5$ and $\alpha = 1/750$ is found to produce the best overall profile as shown in Fig. 3. Thus we conclude that the A state population is non-Boltzmann, peaking at $v' = 5$.

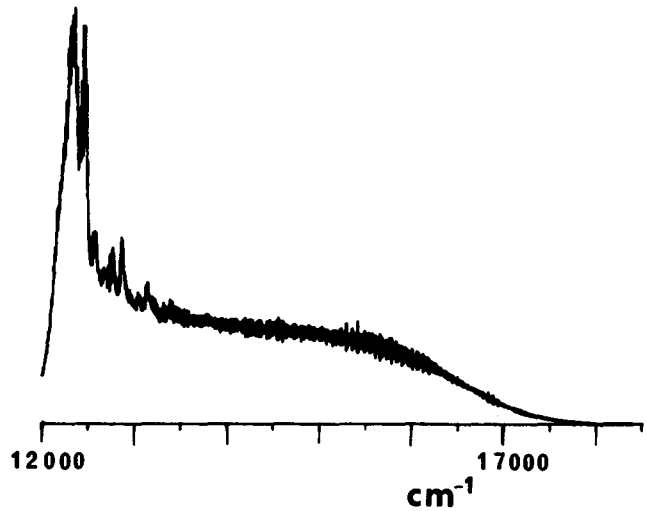

FIG. 3. Simulation of the A–X emission profile using a Gaussian population distribution function centered on $v' = 5$ with $\alpha = 1/750$.

This simulation is, however, crude in the sense that it precludes any knowledge of the mechanism by which the A state is populated. Indeed there is some controversy over this issue, Hulsman and Wilems[18] have obtained data in a molecular beam experiment which suggests that a dissociative/recombination mechanism might be responsible for *some* of the A–X emission, on the other hand, Hussein *et al.*[31] and

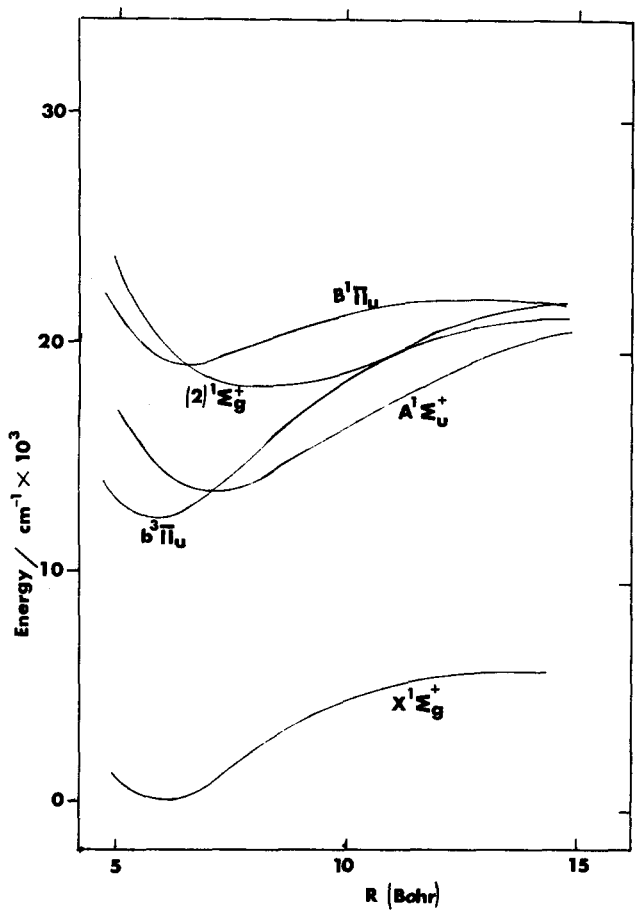

FIG. 4. Adiabatic potential curves of some of the low lying electronic terms in Na_2.

Effantin *et al.*[17] have shown conclusively that radiative transitions from the (2) $^1\Sigma_g^+$ state in the infrared are also responsible for populating the A state. A diagram of the relevant potential energy curves is shown in Fig. 4. At this stage we shall refrain from addressing the question of how the (2) $^1\Sigma_g^+$ state itself becomes populated. The FTIR data measured by Effantin may be used to obtain the vibrational distribution in the (2) $^1\Sigma_g^+$ state. We can then model the infrared fluorescence and from it, deduce the A state population. It is necessary to introduce rotational relaxation in the (2) $^1\Sigma_g^+$ state since the lifetime of the state is such that multicollisional rotational relaxation (cascading) will occur. The lifetime of the (2) $^1\Sigma_g^+$ is not known but can be estimated by assuming an average transition strength equal to the X–A band and taking account of the ν^3 factor. The rotational thermalization of the (2) $^1\Sigma_g^+$ was modeled using the expression derived by Derouard[32];

$$n_i = \frac{s}{\gamma + k}\left[\delta_{ij} + \frac{(1-\delta_{i0})k_{i0}}{\gamma + k} + \sum_{q=1}^{p-1}\left(\frac{\Sigma_{j=0} k_{0j} k_{ji}^{(q)}}{(\gamma + k)^{q+1}}\right)\right], \tag{4}$$

where

$$k_{ij}^{(q)} = \sum_{l \neq j} k_{j \to l} k_{l \to i}^{(q-1)} \tag{5}$$

and

$$k_{j \to i}^{(1)} = k_{j \to i} . \tag{6}$$

Here δ_{ij} is the Dirac delta function, s is the rate of population of the initial state $|0\rangle$, and γ is the rate of spontaneous decay of the initial state. The rate constants $k_{j \to i}$ were modeled using the ECS-P scaling law developed by Pritchard *et al.*[33] The resultant population was then allowed to fluoresce according to Eq. (1), since the variation of the (2) $^1\Sigma_g^+$–A $^1\Sigma_u^+$ dipole moment with internuclear distance was not known. Figure 5 shows the (2) $^1\Sigma_g^+$ state population and the resultant A state distribution following the infrared fluorescence, while Fig. 6 shows the final A–X band simulation. The simulated infrared spectrum was compared with the observed FTIR spectrum and found to be in good agreement. The A state distribution shown in Fig. 5 peaks at $v' = 5$ and has a profile similar to a Gaussian with the addition of a blue tail. This is particularly satisfying in the light of the earlier simulation using a variable width Gaussian centered on $v' = 5$ which produced the best fit to the observed profile. However it should be noted that the width of the Gaussian in the early simulation was much wider than the actual distribution calculated in this simulation which can be approximated by a Gaussian with a width of approximately 1/20. Simulations using a Gaussian of this width reproduce the spectrum shown in Fig. 6 with some degree of success but with the notable absence of the high energy features.

Comparison of the simulation (Fig. 6) with the observed spectrum (Fig. 2) shows excellent agreement around the satellite feature and around the sodium D lines but the correspondence breaks down in the intermediate region between 14 500 and 15 500 cm^{-1}. We address this problem below.

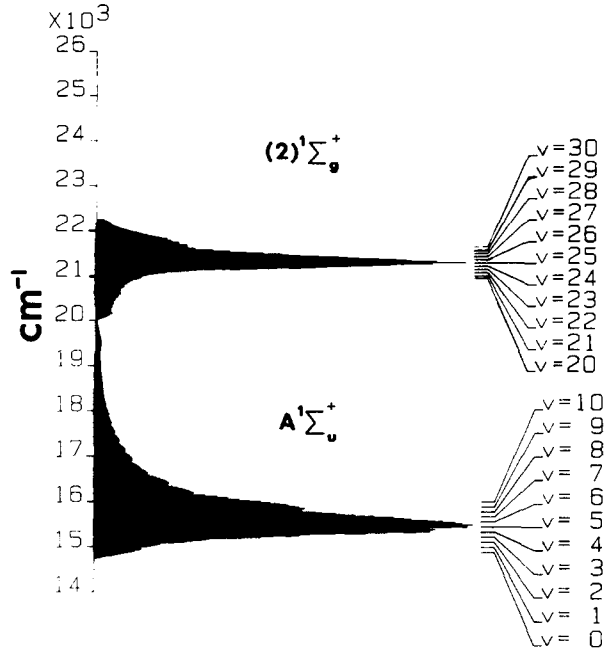

FIG. 5. The (2) $^1\Sigma_g^+$ and A $^1\Sigma_u^+$ population distributions following collisional rotational relaxation in the (2) $^1\Sigma_g^+$ state and subsequent infrared fluorescence to the A $^1\Sigma_u^+$ state.

IV. DISCUSSION

It is clear from the work of Hussein, Effantin, and coworkers that the A state is populated following infrared radiative transitions from the (2) $^1\Sigma_g^+$ state, which is known to cross the initial excited B state. Further support for this comes from our polarization measurements of the A–X fluorescence. For linear excitation the signs of the polarization ratios of the P- and R-branch fluorescent lines are all posi-

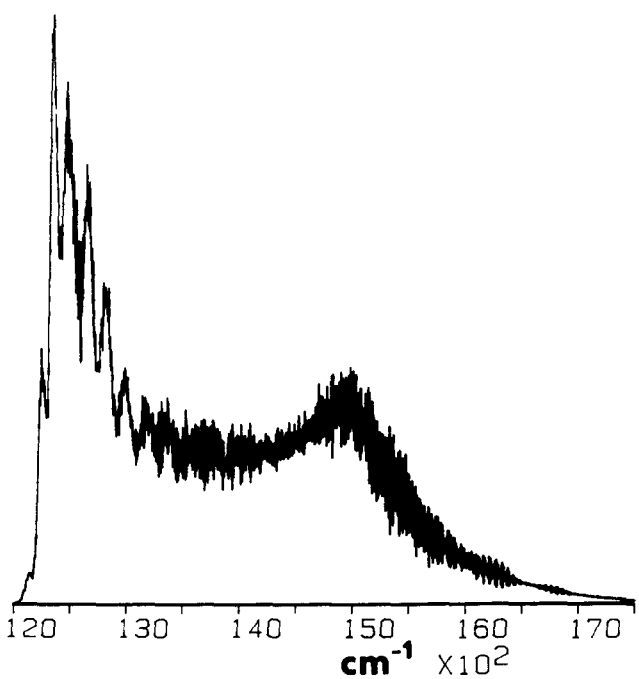

FIG. 6. Simulation of the A–X emission profile using the A state population distribution shown in Fig. 5.

tive, this is true not only for resonance lines but also for levels populated by RET. The observation of negatively polarized light can however be explained as follows. The laser excites $\Sigma \rightarrow \Pi$, a perpendicular transition, the energy is then transferred to the (2) $^1\Sigma_g^+$ state and subsequently fluoresces to the $A\ ^1\Sigma_u^+$ state. The observed $A\ ^1\Sigma_u^+ \rightarrow X\ ^1\Sigma_g^+$ fluorescence is, however, a parallel transition. The net effect therefore is to rotate the polarization vector of the light *provided* that the orientation with respect to the quantization axis (the laser propagation direction **O**) does not change appreciably during the energy transfer. The maximum theoretical polarization ratios for P and R lines (Q transitions are forbidden $\Sigma \rightarrow \Sigma$) are 1/7, so there must be a high propensity to conserve M throughout the $\Pi \rightarrow \Sigma$ crossing to account for the polarization observed in the A–X band.

The computer simulations of the A–X emission are consistent with the nascent vibrational distribution in the (2) $^1\Sigma_g^+$ state obtained from FTIR measurements. The difference between the simulated and observed A–X fluorescence in the region of 14 500–15 500 cm^{-1} can be explained by the presence of the $b\ ^3\Pi_u$ state which crosses and perturbes the A state.[17] The energy at which the maximum perturbation occurs is exactly the same as the energy of the maximum discrepancy. The result of the curve crossing is that states perturbed by the $b\ ^3\Pi_u$ surface are shifted in energy. The resultant A–X transition frequencies and line strengths are hence shifted from their unperturbed (calculated) values. This results in a "smearing" of the spectrum with the destruction of the regular structure observed in other, unperturbed, regions of the band in a manner similar to a quantum interference effect.

We now turn to the mechanism by which the (2) $^1\Sigma_g^+$ state itself becomes populated. Direct radiative transfer between the (2) $^1\Sigma_g^+$ and B states can obviously be ruled out since the energy gap is such that the ν^3 term in the transition probability will be prohibitively small (the lifetime of the $B\ ^1\Pi_u$ state is ≈ 8 ns). The simple gate model of $E \rightarrow E$ energy transfer cannot be invoked since under the operations of the $D_{\infty h}$ point group the non-Born–Oppenheimer terms which might mix the two adiabatic potential surfaces vanish. However the electrostatic interaction with the collision partner may induce mixing between states of different inversion symmetry.

One such model has been proposed by Hussein *et al.*[31] in which the collision is treated by the impact parameter method within the framework of first order time dependent perturbation theory. The interaction potential is a multipolar expansion of the electrostatic moments of the molecule and the colliding atom. The assumed long range nature of the interaction implies that there is no overlap between the wave functions of the molecule and the atom which allows the problem to be separated into atomic and molecular parts. This produces an analytic expression for the transfer probability. The subsequent use of the impact approximation permits the calculation of collision cross sections which are found to be in reasonable agreement with experimental data.

One consequence of the model is that the collision partner has to possess nonzero electronic angular momentum. Thus, Hussein *et al.* conclude that the collision partner must be excited state sodium atom, Na($3\ ^2P$), i.e.,

$$Na_2(B\ ^1\Pi_u) + Na(^2P) \rightarrow Na_2[\,(2)\ ^1\Sigma_g^+\,] + Na(^2P). \tag{7}$$

While we concur that the transfer occurs in the absence of any foreign buffer gas it seems highly improbable that the concentration of excited state sodium atoms in our experiment is large enough to account for the observed A–X intensities. Hussein *et al.* have ignored the spin–orbit interaction in the atomic basis set. Using $J = L + S$ as a good quantum number permits *ground* state sodium atom to induce the crossing via a dipole–dipole coupling terms as opposed to the dipole–quadrupole coupling necessary for the excited state sodium. Such a coupling scheme would be consistent with the model proposed by Carrot *et al.*[34] for the analogous crossing in Li_2. There seems no justification therefore for the assumption that ^2P state Na atoms are responsible for the collision-induced energy transfer.

A more rigorous approach is that of Alexander and Corey[6] in their treatment of $^2\Pi$–$^2\Sigma$ surface crossings in CaO, N_2, N_2^+, and CN. In these systems efficient electronic energy transfer is observed even when the initial and final states are not quasi-isoenergetic and hence conditions for a gate mechanism are not favorable. Furthermore in N_2^+, as well as in Na_2, perturbations mixing states of the two crossing potentials are symmetry forbidden in the isolated molecule. Despite this, however, efficient transfer is observed in both these systems.

In their paper Alexander and Corey[6] make an explicit connection between the electrostatic coupling matrix elements described in the diabatic basis set (i.e., the isolated molecular electronic wave functions) and the appropriate atom–molecule adiabatic wave functions obtained from *ab initio* calculations. The important step in their treatment is the transformation from the three known adiabatic potential surfaces to the four unknown diabatic surfaces using a mixing angle related to the diabatic coupling matrix elements. Significantly this treatment makes no assumptions regarding the range of the interaction potential, unlike the Born approximation employed by Hussein *et al.*[31] The collision dynamics are treated within the fully quantum mechanical close coupled formalism with the colliding atom assumed to be in an S state. Very little is known about the potential energy surfaces of Na_3, although we note recent spectroscopic data,[35] and so a full calculation of the electrostatic coupling matrix elements is beyond our means. However, Alexander and Corey[6] show how the infinite-order sudden (IOS) approximation may be applied to obtain propensity rules and scaling relations which can be checked against the experimental results. This dynamical limit is, of course, the opposite to that invoked by Hussein and co-workers.

For a homonuclear diatomic molecule the permutation-inversion selection rules are rigorous and thus for the $u \leftrightarrow g$ transition present in this system the initial and final vibronic wave functions must be of opposite parity implying that s/a symmetry is conserved. This is obeyed in all three cases reported by Hussein *et al.*,[31] namely $B\ ^1\Pi_u$ ($v = 6$, $J = 43$) $\rightarrow$ (2) $^1\Sigma_g^+$ ($v = 25$, $J = 43$), $B\ ^1\Pi_u$ ($v = 4$, $J = 30$) $\rightarrow$ (2) $^1\Sigma_g^+$ ($v = 20$, 21, 23, $J = 30$) and $B\ ^1\Pi_u$

$(v=7,\ J=43)\rightarrow(2)\ ^1\Sigma_g^+$ $(v=25\text{–}29,\ J=42,44)$. We note that the model developed by Hussein *et al.* predicts a $\Delta J=0,\pm 1$ propensity rule for a dipolar molecular moment which is in agreement with both experimental observations and Alexander and Corey's work, especially in the large J limit. The propensity rules are hence essentially the same in both the Born and IOS limits. In addition the theory described in Ref. 31 predicts a subsequent $\Delta M\leqslant\Delta J$ restriction which is supported by our polarization data.

In the heteronuclear CN radical studied by Dagdigian and co-workers[11–14] electronic energy transfer between Π and Σ states is as efficient as pure RET within the Π state regardless of the degree of non-Born–Oppenheimer mixing between the two adiabatic surfaces. Similar observations in N_2^+ by Katayama[8] lead to the conclusion that $\Delta J\approx 0$ is more important than $\Delta E\approx 0$. Further support for the electrostatic transfer mechanism comes from a reasonable fit of the CN data to the scaling relation derived by Alexander and Corey.[6] Our vibrational state dependence data (Table I) shows little variation in quantum yield with v or B state energy, which tends to suggest that angular momentum considerations are more important than those based on energy-gap or Franck–Condon overlap.

The polarization of the A–X fluorescence provides a strong argument against the mechanism proposed by Hulsman and Wilems[18] involving dissociation and recombination processes. Such pathways are extremely unlikely to preserve the original molecular orientation and hence, we conclude that the electronic energy transfer observed is due to collision induced $B\ ^1\Pi_u\rightarrow(2)\ ^1\Sigma_g^+$ curve crossing. Studies of pure RET suggest that high polarization is associated with a sudden interaction and our observations therefore provide some support for the IOS approach.

The results from the single mode study (Table I) show that the quantum efficiency of the energy transfer from the $B\ ^1\Pi_u\rightarrow A\ ^1\Sigma_u^+$ is about 1% for all of the B state levels sampled. It is surprising that the data do not show any resonances as observed in the FTIR study of the $B\ ^1\Pi_u\rightarrow(2)\ ^1\Sigma_g^+$ curve crossing.[31] At this stage no explanation for this observation can be offered. The data do not correlate to a simple energy gap or gate model. This latter observation again detracts from mechanisms involving dissociative pathways. This is further supported by our earlier work using multimode Ar^+ laser output at 457.9 nm,[16] which showed that no transfer occurred from high lying levels in the B state while at the same time the Na D-line emission increased appreciably. Work currently underway using a continuously tunable dye laser will extend this data set.

V. CONCLUSION

To summarize, our experimental findings of strong emission in the A–X band of Na_2 following laser excitation into single rovibrational states of the $B\ ^1\Pi_u$ state have been shown to be inconsistent with a Boltzmann distribution in the vibrational levels of the A state. Simulations of the spectral profile showed the A state to be vibrationally inverted with the population peaking in the $v'=5$ level. Polarization studies showed that the electronic energy transfer has a high propensity to maintain the alignment of the molecule with respect to the laser propagation direction. Some results have also been presented which measure the relative transfer rates out of individual rovibrational levels in the B state. The quantum efficiency is found to be about 1% for all cases investigated.

Our data has been shown to be consistent with collisionally induced inelastic electronic energy transfer between the $B\ ^1\Pi_u$ and $(2)\ ^1\Sigma_g^+$ states of Na_2, and this has been discussed in the light of propensity rules developed in two dynamical limits (Born and IOS approximations). The collision partner appears to be ^2S state sodium atoms, present with high number density under our experimental conditions. Without state-to-state cross sections for the transfer it is difficult to be quantitative and clearly more work is needed. We are presently trying to obtain state-to-state cross sections in an optical–optical double resonance experiment, the preliminary results of which have been published elsewhere.[36]

ACKNOWLEDGMENTS

We thank the Science and Engineering Research Council for financial support of this work, and for three Research Studentships (AGA, SCT, MJW), and an Advanced Research Fellowship (BJW). We also thank Mr. F. Sondermann for his help on the single mode studies and Mr. C. Jarvis for his excellent technical assistance in the construction of the sodium oven. We would also like to thank Dr. H. Hulsman for some stimulating discussion on this topic and for sending us a copy of his paper prior to publication.

[1] M. H. Alexander, J. Chem. Phys. **76**, 429 (1982).
[2] D. H. Katayama, T. A. Miller, and V. E. Bondybey, J. Chem. Phys. **72**, 5469 (1980).
[3] D. H. Katayama, J. Chem. Phys. **81**, 15 (1984).
[4] M. H. Alexander and M. G. Osmolovsky, J. Chem. Phys. **77**, 839 (1982).
[5] R. W. Field, C. R. Jones, and H. P. Broida, J. Chem. Phys. **60**, 4377 (1974).
[6] M. H. Alexander and G. C. Corey, J. Chem. Phys. **84**, 100 (1986).
[7] D. H. Katayama, J. Chem. Phys. **81**, 3495 (1984).
[8] D. H. Katayama, Phys. Rev. Lett. **54**, 657 (1985).
[9] D. H. Katayama, T. A. Miller, and V. E. Bondybey, J. Chem. Phys. **71**, 1662 (1979).
[10] W. Benesch, J. Chem. Phys. **78**, 2978 (1983).
[11] N. Furio, A. Ali, and P. J. Dagdigian, Chem. Phys. Lett. **125**, 561 (1986).
[12] N. Furio, A. Ali, and P. J. Dagdigian, J. Chem. Phys. **85**, 3680 (1986).
[13] G. Jihua, A. Ali and P. J. Dagdigian, J. Chem. Phys. **85**, 7098 (1986).
[14] A. Ali, G. Jihua, and P. J. Dagdigian, J. Chem. Phys. **87**, 2045 (1987).
[15] G. Ennen and Ch. Ottinger, J. Chem. Phys. **76**, 5812 (1982).
[16] A. G. Astill, A. J. McCaffery, and B. J. Whitaker, Chem. Phys. Lett. **125**, 33 (1986).
[17] C. Effantin, O. Babaky, K. Hussein, J. D'Incan, and R. F. Barrow, J. Phys. B **18**, 4077 (1985).
[18] H. Hulsman and P. Wilems, Chem. Phys. (preprint).
[19] C. Effantin, J. d'Incan, A. J. Ross, R. F. Barrow, and J. Vergès, J. Phys. B **17**, 1515 (1984).
[20] R. A. Shatwell and A. J. McCaffery, J. Phys. E **7**, 299 (1974).
[21] M. L. Janson and J. P. Klavins, Chem. Phys. Lett. **86**, 453 (1982).
[22] H. Hulsman (private communication).
[23] E. W. Rothe, U. Krause, and R. Düren, J. Chem. Phys. **72**, 5145 (1980).
[24] L. K. Lam, T. Fujimoto, A. G. Gallagher, and M. M. Hessel, J. Chem. Phys. **68**, 3553 (1978).
[25] A. N. Nesmeyanov, *Vapor Pressure of the Chemical Elements* (Elsevier, Amsterdam, 1963).
[26] A. Pardo, J. M. L. Poyato, J. I. Fernandez Alonso, and F. R. Rico, Chem. Phys. Lett. **69**, 396 (1980).

[27]R. J. Le Roy, *Further Improved Computer Program for Solving the Radial Schrödinger Equation for Bound and Quasibound (Orbiting Resonance) Levels* (University of Waterloo, Waterloo, 1985).
[28]W. J. Stevens, M. M. Hessel, D. J. Bertoncini, and A. C. Wahl, J. Chem. Phys. **66**, 1477 (1977).
[29]P. Kusch and M. M. Hessel, J. Chem. Phys. **68**, 2591 (1978).
[30]M. E. Kaminsky, J. Chem. Phys. **66**, 4987 (1977); **73**, 3520(E) (1980).
[31]K. Hussein, M. Aubert-Frécon, O. Babaky, J. D'Incan, C. Effantin, and J. Vergès, J. Mol. Spectrosc. **114**, 105 (1985).
[32]J. Derouard, Ph.D. thesis, Université Scientifique et Medicale de Grenoble, 1983.
[33]N. Smith and D. E. Pritchard, J. Chem. Phys. **74**, 3939 (1981).
[34]F. Carrot, M. Aubert-Frécon, R. Bacis, S. Churassy, and J. Vergès, Phys. Rev. Lett. **57**, 420 (1986).
[35]M. Broyer, G. Delacrétaz, P. Labastie, R. L. Whetten, J. P. Wolf, and L. Wöste, Z. Phys. D **3**, 131 (1986).
[36]A. G. Astill, A. J. McCaffery, and B. J. Whitaker, Chem. Phys. Lett. **142**, 1 (1987).